

Temporal dissipative solitons in time-delay feedback systems

Serhiy Yanchuk¹, Stefan Ruschel¹, Jan Sieber², Matthias Wolfrum³

¹*Institute of Mathematics, Technical University of Berlin, Strasse des 17 Juni 136, 10623 Berlin, Germany*

²*Harrison Building, North Park Road, CEMPS University of Exeter, Exeter, EX4 4QF, UK and*

³*Weierstrass Institute, Mohrenstrasse 39, 10117 Berlin, Germany*

Localized states are a universal phenomenon observed in spatially distributed dissipative nonlinear systems. Known as dissipative solitons, auto-solitons, spot or pulse solutions, these states play an important role in data transmission using optical pulses, neural signal propagation, and other processes. While this phenomenon was thoroughly studied in spatially extended systems, temporally localized states are gaining attention only recently, driven primarily by applications from fiber or semiconductor lasers. Here we present a theory for temporal dissipative solitons (TDS) in systems with time-delayed feedback. In particular, we derive a system with an advanced argument, which determines the profile of the TDS. We also provide a complete classification of the spectrum of TDS into interface and pseudo-continuous spectrum. We illustrate our theory with two examples: a generic delayed phase oscillator, which is a reduced model for an injected laser with feedback, and the FitzHugh-Nagumo neuron with delayed feedback. Finally, we discuss possible destabilization mechanisms of TDS and show an example where the TDS delocalizes and its pseudo-continuous spectrum develops a modulational instability.

Solitons have been known as a physical phenomenon from the early 19th century [1]. They are commonly associated with spatially localized states in conservative spatially extended systems, such as the Korteweg-de Vries or the nonlinear Schrödinger equation and possess remarkable properties such as preservation of localization and shape after collisions. Beyond the “classical” conservative solitons, localized states were also observed in earlier works on non-conservative chemical and physiological systems, see [2] and references therein.

Interest in localized solutions of non-conservative and non-integrable systems has grown rapidly since the early 1990s [2–9]. These states have been called dissipative solitons (DS). In contrast to conservative solitons, DS are stable objects (attractors), which emerge due to a nonlinear balance between energy gain and loss [8]. DS have been discovered in spatially extended systems modeled by partial differential equations in optics [3, 5, 7, 8, 10–12], biological systems [3, 13–15], plasma physics [3, 16] and other fields [17].

Recent experimental and theoretical results report that DS are also possible in systems with time-delayed feedback that do not include explicit spatial variables [18–27]. In these systems the time delay is larger than the other timescales and the DS are temporally localized. Their natural relation to spatially localized states can be seen in a spatio-temporal representation of the dynamics of time-delayed systems as done in [28, 29]. In this representation the pulse is localized within the *delay line*. For example, in a ring laser this delay line corresponds physically to the ring cavity, where the optical pulse is localized [18].

Examples of systems exhibiting temporal DS (TDS) include opto-electronic setups such as mode-locked lasers with saturable absorber [18, 19, 27], coupled broad-area semiconductor resonators [30], vertical-cavity surface-emitting lasers with delays [21], as well as neuronal models [23] or bistable systems with feedback [20, 24]. Although localized states have been reported mainly in one dimension, two-dimensional TDS have been found as well for a system with two feedback loops [25]. In this case the lengths of the delays were significantly different. Then one can associate one spatial dimension to each delay line, thus representing the temporal dynamics using

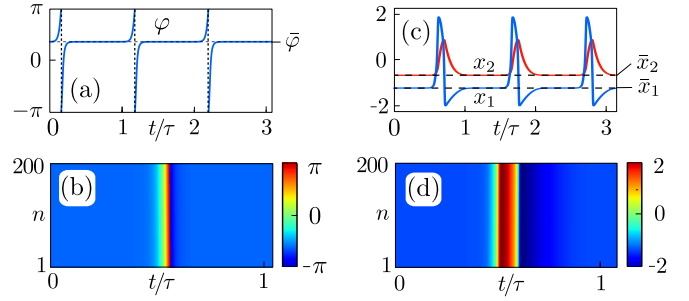


Figure 1. Examples of temporal dissipative solitons (TDS) in the delayed phase oscillator (2) (a,b) and FHN system (3) (c,d). Panels (a,c) show the time profiles $\varphi(t)$ and $x(t)$ and (b,d) their spatio-temporal representations. The spatio-temporal representation shows the solutions $\varphi(t)$ in (b) (and $x_1(t)$ in (d)) as color plot with respect to the pseudo-spatial variable (delay-line) along the horizontal axis ($t/\tau \bmod T/\tau$) and the pseudo-temporal variable (number of round-trips) along the vertical axis ($n = [t/T]$) [28, 29]. Parameter values: (a,c) $d = 0.9, \kappa = 1, \tau = 40$, (b,d) $a = 0.7, b = 0.8, \kappa = 0.1, \varepsilon = 0.08, \tau = 100$.

a two-dimensional spatial representation [31, 32]. Localized states can have different forms. For instance, they can be composed of several pulses, known as soliton molecules or bound states [21, 26, 33]. Experimental and theoretical methods to control the nucleation or cancellation of TDS have been introduced in [22, 23].

Considering the importance of TDS in systems with delayed feedback, their variety and broadness of applications, there is a need for a unifying theory describing basic properties of TDS. In this Letter, we outline such a theory for TDS with a stable equilibrium *background state* (see Fig. 1 for typical time profiles) for general systems with delayed feedback of the form

$$\dot{x}(t) = f(x(t), x(t - \tau)), \quad (1)$$

where $x(t) \in \mathbb{R}^n$ is a variable describing the state of the system, τ is the large feedback delay, and $f(\cdot, \cdot)$ is a nonlinear function determining the dynamics.

We present two ingredients that enable TDS to emerge in

systems (1), and introduce an equation describing the TDS time profile. Using the largeness of time delay τ , we describe the spectrum of Floquet multipliers of TDS. This spectrum consists of two parts. The first is the *pseudo-continuous spectrum* (PCS), determined entirely by (but not equal to) the spectrum of its background state. We provide an explicit expression for the PCS when the time-delayed feedback has rank 1 and a simple description for PCS computation otherwise. The second part is a point (or *interface*) spectrum, for which we provide an asymptotic approximation that is independent of the large delay τ and hence can be evaluated numerically (a corresponding tool is provided for DDE-Biftool [34]). The obtained results predict possible destabilization mechanisms of TDS. We specify these mechanisms and conclude by showing an example of delocalization of TDS and the development of a modulational instability.

Examples of TDS are shown in Fig. 1 for the delayed phase oscillator

$$\dot{\varphi} = d - \sin \varphi + \kappa \sin(\varphi(t - \tau) - \varphi), \quad (2)$$

and the FitzHugh-Nagumo (FHN) neuron with delayed feedback

$$\begin{aligned} \dot{x}_1 &= x_1 - (x_1^3/3) - x_2 + \kappa x_1(t - \tau), \\ \dot{x}_2 &= \varepsilon(x_1 + a - bx_2). \end{aligned} \quad (3)$$

System (2) is a reduced model for a general injected Ginzburg-Landau equation with delayed feedback [22] (see Fig. 1 for parameters).

We observe that TDS are periodic solutions with a period T slightly larger than the time delay τ . We denote $T = \tau + \delta$ where $\delta \ll \tau$ will remain bounded as τ gets large. As Fig. 1 shows, the solutions spend most of the time close to a constant stationary state \bar{x} , which we call the *background*.

Conditions for the emergence of TDS and profile equation. The first ingredient is the existence of a background equilibrium \bar{x} that is stable for arbitrary long delay τ . The equilibrium \bar{x} satisfies $f(\bar{x}, \bar{x}) = 0$. It is stable if all roots λ of the characteristic equation $\det(\lambda I - A_0 - B_0 \exp(-\lambda\tau)) = 0$ have negative real parts [35]. Here $A_0 = \partial_1 f(\bar{x}, \bar{x})$ and $B_0 = \partial_2 f(\bar{x}, \bar{x})$ are Jacobians of the function f with respect to the first and second argument, respectively, evaluated at \bar{x} . Interestingly, stability of the background for long delays implies its stability for arbitrary positive delays τ including small and zero delay [36]. Explicit stability criteria for large delays τ are given in [37].

The second ingredient refers to the time profile $s(t)$ of the TDS. Using its $T = \tau + \delta$ -periodicity, we find that $s(t)$ satisfies (1) if and only if

$$\dot{s}(t) = f(s(t), s(t + \delta)) \quad (4)$$

since $s(t - \tau) = s(t - \tau + T) = s(t + \delta)$. In the resulting *profile equation* (4), where the large time delay is replaced by a finite positive time shift δ , the TDS appears as a family of periodic solutions with long periods that for some positive $\delta = \delta_h$ approaches a *connecting orbit* (also called homoclinic solution) $s_h(t)$ to \bar{x} . We recall that a connecting orbit satisfies $s_h(t) \rightarrow \bar{x}$ for $t \rightarrow \pm\infty$, i.e. it approaches the background \bar{x} forward and

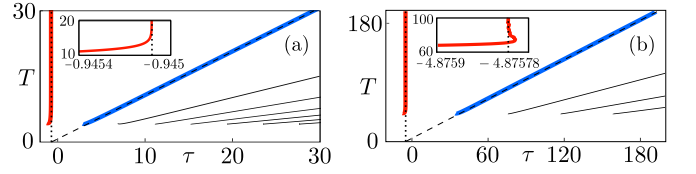


Figure 2. Branches of periodic solutions: (a) delayed phase oscillator (2); (b) FHN system (3); period T versus delay τ . The primary branch of TDS (solid blue curves) has the asymptotic period $T = \tau + \delta_h$ (dashed line). The branch reappears for negative delays $-\delta = \tau - T$ (red lines) and limits to the connecting orbit of the profile equation (4) with $\delta \rightarrow \delta_h$ and $T \rightarrow \infty$ (dotted line). Higher harmonic TDS branches (black lines) correspond to the branches reappearing with time-delays $\tau + kT(\tau)$ (multiple solitons per delay interval). Other parameters: (a) $d = 0.9, \kappa = 0.9$ (b,d) $a = 0.7, b = 0.8, \kappa = 0.1, \varepsilon = 0.08$.

backward in time. Clearly, such an orbit cannot exist for negative δ because the background \bar{x} is stable in (1). Another reason for the positive sign of δ_h is the causality principle [29] which implies that the period of a stable TDS is larger than the time-delay τ .

The homoclinic solution $s_h(t)$ of the profile equation (4) with $\delta = \delta_h$ implies the appearance of TDS in system (1) for large delays τ in the following way. Considering δ as a parameter in (4), the general theory for connecting orbits [38] guarantees that for δ close to δ_h , the profile equation possesses a family of periodic solutions $s_\delta(t)$ with periods T_δ approaching infinity as $\delta \rightarrow \delta_h$. These periodic solutions converge to the connecting orbit with infinite period as $\delta \rightarrow \delta_h$. Using the periodicity, we have $s_\delta(t + \delta) = s_\delta(t + \delta - T_\delta) = s_\delta(t - \tau)$ with $\tau = T_\delta - \delta$. Hence, $s_\delta(t)$ solves (1) with $\tau = T_\delta - \delta$. Since T_δ goes to infinity, the branch of periodic solutions $s_\delta(t)$ of the original system (1) also exists for the large time delay $\tau = T_\delta - \delta$ with $\tau \rightarrow \infty, \delta \rightarrow \delta_h$. Moreover, the solutions s_δ are close to the connecting orbit, and hence, they are TDS.

In short, the main ingredients leading to TDS are:

- (A) A background equilibrium \bar{x} that is stable for large and, hence, also for arbitrary positive delays.
- (B) The profile equation (4) possesses a connecting orbit to \bar{x} for some positive value δ_h . The period of the TDS is then approximately $T \approx \tau + \delta_h$ for large delays.

The profile equation (4) is a differential equation with an advanced argument. This is in contrast to the profile equations for spatial DS [2–8], which are ordinary differential equations.

The bifurcation diagram in Fig. 2 illustrates the relation between the solutions of the profile equation (red branch) and the TDS solutions (blue branch), showing the periods as a function of the time-delay τ . One can clearly see the asymptotic behavior $T \approx \tau + \delta_h$ for the period along the blue primary stable branch of TDS. The branches are related by the general reappearance rule $\tau_k = \tau + kT(\tau)$, see [39], where $k = 0$ corresponds to the blue branch, $k = -1$ to the red, and $k > 2, 3, \dots$ to the higher harmonic branches (black). The defining feature for TDS is that the period along the red branch diverges, and that the periodic solutions approach the connecting orbit $s_h(t)$ as $\tau \rightarrow -\delta_h$.

Spectrum of TDS and mechanisms for its destabilization.

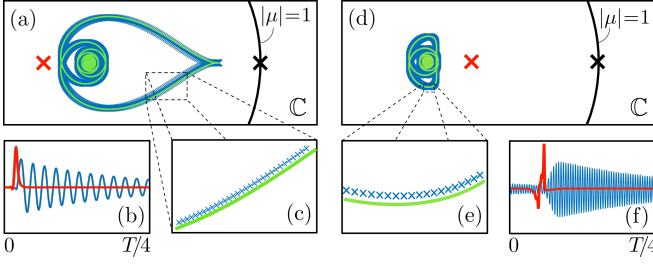


Figure 3. Spectrum and eigenfunctions of TDS: (a)-(c) delayed phase oscillator (2); (d)-(f) FHN system (3). Panels (a),(d) with zoomed parts in panels (c), (e) show numerically computed multipliers (crosses) and the approximating curves (9) and (10) for the PCS (green curves). Interface spectrum (red and black crosses) can be computed using the Evans function (8). Eigenfunctions in panels (b), (f): Localized profiles (red) correspond to interface spectrum; non-localized profiles (blue) correspond to PCS. Parameters for (a)-(c): $d = 0.9, \kappa = 0.9, \tau = 200$; for (d)-(f): $a = 0.7, b = 0.8, \kappa = 0.1, \varepsilon = 0.08, \tau = 1000$.

Next we describe the spectrum of TDS, which determines the stability, possible bifurcations and destabilization scenarios of TDS. We show that the spectrum has two parts: *pseudo-continuous* (PCS) and *interface* spectrum, see Fig. 3. The PCS is determined by the background while the interface spectrum consists of usually only few relevant multipliers that are determined by the profile properties.

To determine its spectrum, system (1) is linearized around the TDS solution $s_\delta(t)$:

$$\dot{y}(t) = A(t)y(t) + B(t)y(t - \tau), \quad (5)$$

where $A(t) = \partial_1 f(s_\delta(t), s_\delta(t + \delta))$ and $B(t) = \partial_2 f(s_\delta(t), s_\delta(t + \delta))$. Taking into account the properties of TDS, the coefficients $A(t)$ and $B(t)$ are most of the time exponentially close to A_0 and B_0 , respectively, except for intervals of length of order 1 where the TDS is different from the background.

A solution $y(t)$ of (5) provides an eigenfunction with characteristic multiplier μ if $y(t + T) = \mu y(t)$. Using the equality $y(t - \tau) = \mu^{-1} y(t - \tau + T) = \mu^{-1} y(t + \delta)$ we obtain the eigenvalue problem

$$\dot{y}(t) = A(t)y(t) + \mu^{-1} B(t)y(t + \delta), \quad y(t + T) = \mu y(t) \quad (6)$$

for the eigenfunctions y and multipliers μ . For stable TDS all multipliers have $|\mu| < 1$, except the trivial one $\mu = 1$ corresponding to the time-shift.

Our goal is to find approximations of the solutions $y(t)$ and μ of the eigenvalue problem (6). Without loss of generality, the soliton localization region can be moved to the origin, such that $x(t) \approx \bar{x}$, $A(t) \approx A_0$ and $B(t) \approx B_0$ for $1 \ll |t| < T/2$. Hence, the asymptotics of $y(t)$ for large $|t|$ is governed by the roots of the characteristic equation for (6) with constant coefficients,

$$\det \Delta(\mu, \rho) = \det (\rho I - A_0 - \mu^{-1} e^{\rho \delta} B_0) = 0. \quad (7)$$

We distinguish two types of multipliers μ : interface spectrum, for which the characteristic equation (7) possesses no

purely imaginary roots $\rho = i\omega$, and PCS, where (7) has such purely imaginary roots.

Interface spectrum. It is known that systems with advanced arguments $\delta > 0$ possess at most finitely many stable eigenvalues, i.e. roots ρ_j , $j = 1, \dots, k_s$ of Eq. (7) with negative real parts. Assuming that there are no imaginary roots $\rho = i\omega$, we conclude that all solutions $y(t)$ of (6) that do not diverge for large $t > 0$, decay exponentially with possible rates ρ_j . Thus, $y(t)$ must have the form $y(t_L + \theta) \approx \sum_{j=1}^{k_s} c_j v_j \exp(\rho_j(t_L + \theta))$ for any large positive time t_L , where the coefficients c_j are arbitrary and to be determined below, v_j are the eigenvectors satisfying $\Delta(\mu, \rho_j)v_j = 0$, and $0 \leq \theta \leq \delta$.

Starting from such a state $y(t_L + \theta)$, system (6) can be integrated backward until the negative large time $-t_L$. Since the system is linear, this corresponds to a certain linear transformation $y(-t_L + \theta) = [M]y(t_L + \theta) = \sum_{j=1}^{k_s} c_j M v_j \exp(\rho_j(t_L + \theta))$. The obtained function $y(-t_L + \theta)$ must be orthogonal to all stable eigenfunctions $v_j \exp(\rho_j \theta)$, otherwise it will diverge for large negative time. This orthogonality is with respect to the pairing $\langle w_k | y \rangle = w_k^H y(0) - \mu^{-1} \int_0^\delta w_k^H B_0 \exp(\rho_k(\delta - s)) y(s) ds$, where we use the adjoint eigenvectors w_k satisfying $w_k^H \Delta(\mu, \rho_k) = 0$. Then the orthogonality conditions are $\langle w_k | y(-t_L + \theta) \rangle = 0$ for $k = 1, \dots, k_s$. Defining $c = (c_1, \dots, c_{k_s})$ and the $k_s \times k_s$ square matrix $E(\mu)$ with entries $E_{kj} = \langle w_k | M v_j \exp(\rho_j \theta) \rangle$, the latter orthogonality condition can be written in matrix form as $E(\mu)c = 0$. The obtained system possesses nontrivial solutions if

$$\det E(\mu) = 0, \quad E_{kj} = \langle w_k | M v_j e^{\rho_j \theta} \rangle, \quad (8)$$

which is the equation for the interface spectrum.

All elements of the matrix E are defined independently of the large delay τ or period T . The operator M corresponding to the linear evolution across the interface from t_L to $-t_L$ is the only part to be computed numerically. The function given by Eq. (8) has the same structure as the Evans functions for localized solutions in spatially extended systems [5, 40]. An algorithm for computing the interface spectrum using the presented theory is implemented in the software DDE-Biftool [34]. Figure 3 shows examples of the interface spectrum (red and black crosses in panels (a) and (d)). According to our construction the corresponding eigenfunctions $y(t)$ in Fig. 3 are localized at the interface and decay exponentially to zero in the background region of the TDS (red profiles in panels (b) and (f)).

Pseudo-continuous spectrum (PCS) (blue crosses in Fig. 3) is given by multipliers μ , for which the characteristic equation (7) has purely imaginary roots $\rho_c = i\omega$. Substituting $\rho = i\omega$ in (7), we obtain $\det \Delta(\mu, i\omega) = \det (i\omega I - A_0 - \mu^{-1} e^{i\omega \delta} B_0) = 0$. This relation determines a curve $\mu(\omega)$ in the complex plane (green curves in Fig. 3), along which the multipliers μ of the PCS accumulate. For scalar systems this curve has the form $\mu(\omega) = e^{i\omega \delta} B_0 / (i\omega - A_0)$, which gives for (2)

$$\mu(\omega) = \kappa e^{i\omega \delta_h} / (i\omega + \cos \bar{\varphi} + \kappa). \quad (9)$$

In systems with more variables, the equation $\det \Delta(\mu, i\omega) = 0$

is a polynomial of degree rank B_0 in μ^{-1} . In the FitzHugh-Nagumo system (3) the feedback is scalar (rank $B_0 = 1$), giving

$$\mu(\omega) = \kappa(\varepsilon b + i\omega)e^{i\omega\delta_h} / (\varepsilon + (\bar{x}_1^2 + i\omega - 1)(\varepsilon b + i\omega)). \quad (10)$$

The imaginary root $\rho_c = i\omega$ of Eq. (7) implies that the eigenfunction $y(t)$ of the corresponding multiplier $\mu(\omega)$ is a multiple of $v_0 e^{i\omega t}$ far from the interface soliton for $1 \ll |t|$ (v_0 is the nullvector of $\Delta(\mu(\omega), i\omega)$) and hence, in contrast to the eigenfunctions of the interface spectrum, it is not localized (blue profiles in Figs. 3(b),(f)).

The presented theory allows a detailed study of TDS in any system with delayed feedback of the form (1). While delay systems with large delay are typically characterized by high dimensional dynamics, our approach of separating the large timescale of delay from the short timescale of the soliton interface allows to find the soliton profile and the interface spectrum from the desingularized equations (4) and (8) independently of the large delay. Indeed, the interface spectrum describes the linear response with respect to variations of the shape and position of the soliton interface. Corresponding instabilities are induced by isolated multipliers and can be studied within the classical framework of low-dimensional systems, leading to e.g. period-doubled or quasiperiodically modulated TDS. Moreover, on the level of the profile equation (4), the bifurcations of the TDS can be related to the theory of homoclinic bifurcations [38]. Note that classical codimension-two homoclinic bifurcations (e.g. orbit flip, inclination flip, or Shilnikov type) appear here already under the variation of a single control parameter of (1), since the time shift δ appears as an additional unfolding parameter in (4). However, as soon as the background equilibrium ceases to be hyperbolic the high dimensional nature of the system comes into play. Similarly to the critical continuous spectrum at background instabilities of spatially extended systems, PCS approaching the unit circle describes the corresponding phenomenon for TDS.

We conclude with an example showing that in such situations specific new dynamical scenarios have to be expected. In Fig. 4 we study numerically the destabilization of TDS in the phase oscillator system (2) as the excitability parameter d changes. With increasing d , the background equilibrium $\bar{\varphi}$, given by $d = \sin \bar{\varphi}$, disappears in a saddle-node bifurcation at $d = 1$, see Fig. 4(a). At the same time, the PCS touches the imaginary axis and the localization of the phase soliton becomes no more exponential.

Despite of the disappearance of the background, there is still a stable localized periodic solution, spending most of its period in the region where the background equilibrium has vanished. Such a state exists within a small parameter interval of order $1/\tau$. Strictly speaking, it is no more a TDS, as the “ghost” of the saddle-node equilibrium serves as the new background for

this state. Indeed, after the background equilibrium vanishes, orbits still slow down in the region of the phase space of the profile equation where the equilibrium formerly existed. If the time spent in the ghost region is longer than the time-delay, the ghost region can effectively serve as the background.

Following this periodic branch further, the period becomes slightly smaller than the delay and the solution loses its sta-

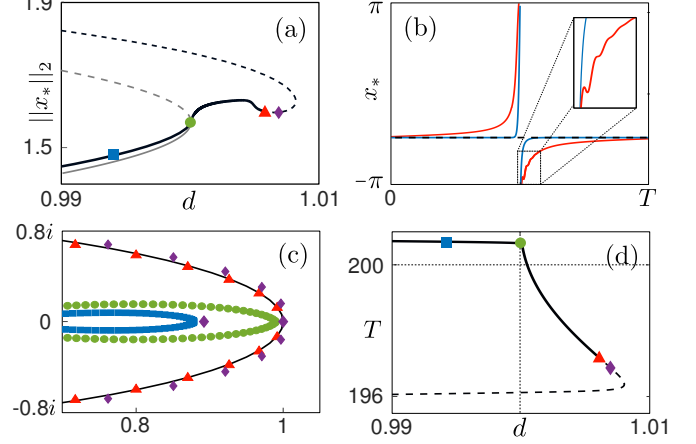


Figure 4. Delocalization and development of modulational instability of a TDS in system (2). (a) solution branches of the background steady state (gray) and the periodic solution (black) versus the excitability parameter d . Numerically obtained Floquet spectra (c) and profiles (b) of selected periodic solutions, indicated by points of corresponding color in (a). Panel (d) shows period versus d . Other parameters $\kappa = 0.9$, $\tau = 200$.

bility. This instability involves a large number of multipliers, which originate from the former PCS and create a destabilization scenario similar to a modulational instability. Finally, the branch turns back into the region $d < 1$, now as a highly unstable soliton solution, which is attached to an unstable background equilibrium.

For this and other TDS destabilization scenarios our theory provides a systematic framework, which can be considered as a substantial extension of the classical theory for dissipative solitons in spatially extended systems.

ACKNOWLEDGMENTS

Financial support acknowledgments. SY: Deutsche Forschungsgemeinschaft (DFG, project 411803875); JS: EP-SRC via grants EP/N023544/1 and EP/N014391/1, and European Union’s Horizon 2020 research and innovation programme under the Marie Skłodowska-Curie grant agreement No 643073; SR: IRTG 1740/TRP 2015/50122-0, funded by DFG/FAPESP; MW and SR: Deutsche Forschungsgemeinschaft (DFG, project number 163436311, SFB 910).

- 59, 485 (2010).
- [3] B. S. Kerner and V. V. Osipov, *Autosolitons* (Springer Netherlands, Dordrecht, 1994) p. 671.
 - [4] N. N. Rosanov, *Spatial Hysteresis and Optical Patterns*, Springer Series in Synergetics (Springer Berlin Heidelberg, Berlin, Heidelberg, 2002).
 - [5] N. N. Akhmediev and A. Ankiewicz, *Dissipative Solitons*, edited by N. Akhmediev and A. Ankiewicz, Lecture Notes in Physics, Vol. 661 (Springer Berlin Heidelberg, Berlin, Heidelberg, 2005) p. 448.
 - [6] N. N. Akhmediev and A. Ankiewicz, *Dissipative Solitons: From Optics to Biology and Medicine*, Lecture Notes in Physics, Vol. 751 (Springer Berlin Heidelberg, Berlin, Heidelberg, 2008) p. 477.
 - [7] T. Ackemann, W. J. Firth, and G. L. Oppo, in *Adv. At. Mol. Opt. Phys.*, edited by P. R. B. E. Arimondo and C. C. Lin (Academic Press, 2009) Chap. 6, pp. 323–421.
 - [8] P. Grelu and N. Akhmediev, *Nat. Photonics* **6**, 84 (2012).
 - [9] P. Parra-Rivas, D. Gomila, M. A. Matías, and P. Colet, *Phys. Rev. Lett.* **110**, 064103 (2013).
 - [10] S. Barland, J. R. Tredicce, M. Brambilla, L. A. Lugiato, S. Balle, M. Giudici, T. Maggipinto, L. Spinelli, G. Tissoni, T. Knödl, M. Müller, and R. Jäger, *Nature* **419**, 699 (2002).
 - [11] J. K. Jang, M. Erkintalo, S. G. Murdoch, and S. Coen, *Nat. Photonics* **7**, 657 (2013).
 - [12] A. Bednyakova and S. K. Turitsyn, *Phys. Rev. Lett.* **114**, 113901 (2015).
 - [13] T. Heimburg and A. D. Jackson, *Proc. Natl. Acad. Sci.* **102**, 9790 (2005).
 - [14] B. Lautrup, R. Appali, A. D. Jackson, and T. Heimburg, *Eur. Phys. J. E* **34**, 57 (2011).
 - [15] E. Villagran Vargas, A. Ludu, R. Hustert, P. Gumrich, A. D. Jackson, and T. Heimburg, *Biophys. Chem.* **153**, 159 (2011).
 - [16] A. V. Tur, A. V. Chechkin, and V. V. Yanovsky, *Phys. Fluids B Plasma Phys.* **4**, 3513 (1992).
 - [17] H. H. Rotermund, S. Jakubith, A. von Oertzen, and G. Ertl, *Phys. Rev. Lett.* **66**, 3083 (1991).
 - [18] A. G. Vladimirov and D. Turaev, *Phys. Rev. A* **72**, 033808 (2005).
 - [19] M. Marconi, J. Javaloyes, S. Balle, and M. Giudici, *Phys. Rev. Lett.* **112**, 223901 (2014).
 - [20] F. Marino, G. Giacomelli, and S. Barland, *Phys. Rev. Lett.* **112**, 103901 (2014).
 - [21] M. Marconi, J. Javaloyes, S. Barland, S. Balle, and M. Giudici, *Nat. Photonics* **9**, 450 (2015).
 - [22] B. Garbin, J. Javaloyes, G. Tissoni, and S. Barland, *Nat. Commun.* **6**, 5915 (2015).
 - [23] B. Romeira, R. Avó, J. M. L. Figueiredo, S. Barland, and J. Javaloyes, *Sci. Rep.* **6**, 19510 (2016).
 - [24] V. V. Semenov and Y. L. Maistrenko, *Chaos An Interdiscip. J. Nonlinear Sci.* **28**, 101103 (2018).
 - [25] D. Brunner, B. Penkovsky, R. Levchenko, E. Schöll, L. Larger, and Y. Maistrenko, *Chaos An Interdiscip. J. Nonlinear Sci.* **28**, 103106 (2018).
 - [26] X. Liu, X. Yao, and Y. Cui, *Phys. Rev. Lett.* **121**, 023905 (2018).
 - [27] C. Schelte, J. Javaloyes and S. Gurevich, *Phys. Rev. A* **97**, 053820 (2018).
 - [28] G. Giacomelli and A. Politi, *Phys. Rev. Lett.* **76**, 2686 (1996).
 - [29] S. Yanchuk and G. Giacomelli, *J. Phys. A Math. Theor.* **50**, 103001 (2017).
 - [30] P. Genevet, S. Barland, M. Giudici, and J. R. Tredicce, *Phys. Rev. Lett.* **101**, 123905 (2008).
 - [31] S. Yanchuk and G. Giacomelli, *Phys. Rev. Lett.* **112**, 174103 (2014).
 - [32] S. Yanchuk and G. Giacomelli, *Phys. Rev. E* **92**, 042903 (2015).
 - [33] D. Puzyrev, A. G. Vladimirov, A. Pimenov, S. V. Gurevich, and S. Yanchuk, *Phys. Rev. Lett.* **119**, 163901 (2017).
 - [34] J. Sieber, K. Engelborghs, T. Luzyanina, G. Samaey, and D. Roose, (2014), arXiv:1406.7144.
 - [35] J. K. Hale, *Theory of Functional Differential Equations* (Springer-Verlag, 1977) p. 365.
 - [36] If \mathfrak{K} is unstable for some delay $\tau_0 > 0$, then there must be a bifurcation for the larger value $\tau_b > \tau_0$ where $\lambda = i\omega$ is purely imaginary, and, hence, $i\omega I - A - B e^{i\omega\tau_b} = 0$. The latter equality implies that $i\omega I - A - B e^{i\omega\tau_k} = 0$ for all delays $\tau_k = \tau_b + 2\pi k/\omega$ with arbitrary integer k , thus, contradicting to the stability for long delays.
 - [37] M. Lichtner, M. Wolfrum, and S. Yanchuk, *SIAM J. Math. Anal.* **43**, 788 (2011).
 - [38] L. P. Shilnikov, A. L. Shilnikov, D. V. Turaev, and L. O. Chua, *Methods of Qualitative Theory in Nonlinear Dynamics*, World Scientific Series on Nonlinear Science Series A, Vol. 5 (World Scientific, 2001).
 - [39] S. Yanchuk and P. Perlikowski, *Phys. Rev. E* **79**, 046221 (2009).
 - [40] B. Sandstede, in *Handb. Dyn. Syst. II*, edited by B. Fiedler (North-Holland, Amsterdam, 2002) Chap. Stability, pp. 983–1055.